Geometric and electronic structure of Pd/4-aminothiophenol/Au(111) metal-molecule-metal contacts: a periodic DFT study

Jan Kučera and Axel Groß
Institute for Theoretical Chemistry, Ulm University, D-89069 Ulm/Germany

Periodic density functional theory calculations were performed to address the geometric and electronic structure of a Pd/4-aminothiophenol/Au(111) metal-molecule-metal contact. In a systematic approach, we first determined the adsorption of single 4-aminothiophenol (4-ATP) molecules on Au(111). Like other aromatic molecules, 4-ATP molecules adsorb preferentially at near-bridge sites in a tilted configuration. Since self-assembled monolayers (SAMs) are typically prepared in an aqueous environment, we also studied the interaction of water with 4-ATP finding a negligible influence of water on the 4-ATP/Au(111) bonding. A Pd monolayer is only weakly bound to an intact 4-ATP double layer on Au(111) via a single Pd-NH_2 bond. However, the strong H-Pd interaction induces the dehydrogenation of the amino group which results in a much stronger 4-ATP-Pd bonding. This also causes a drastic decrease of the local density of states near the Fermi energy and a down-shift of the d-band, in good agreement with the experiment. Strongly bound sulfur- and nitrogen-containing adsorbates on top of the Pd layer would also lead to a decrease in the density of states at the Fermi energy.

I. INTRODUCTION

Self-assembled monolayers (SAMs) of nitrogen containing aromatic thiolates on gold have been proposed as a fundamental element for nanoelectronic devices [1–3]. Such aromatic molecules are typically bound *via* their sulfur head group to gold electrodes and form well-organized self-assembled layers [4–6]. If the molecule contains nitrogen on the opposite tail, as *e.g.* in 4-mercaptopyridine (4-Mpy) or 4-aminothiophenol (4-ATP), an additional layer of metal atoms such as Pd or Pt can be deposited on top of the SAM [2, 3, 7–10] and thus form a metal/SAM/metal junction (M/SAM/M). Such a junction can serve as a model system for studying the transport through molecular electronic devices in order to understand metal-molecule interfacial phenomena in man-tailored nanoelectronics [2, 3]. Just recently, even the preparation of a "double decker" Au/SAM/M/SAM/M structure has been demonstrated [11] showing that the controlled organization of multiple molecular layers and appropriate metal interlayers as intermediate electrodes is possible.

However, the preparation of these M/SAM/M structures requires considerable care, and also the characterization of such complexes suffers ambiguities as far as the interpretation of the experimental results is concerned. The difficulties in the preparation are due to the fact that it is energetically much more favorable for the deposited metal atoms to bind to the metal support rather than to the organic layer. The pioneering work demonstrating the feasibility of the electrochemical metallization of a SAM was performed by Baunach *et al.* for the Au/SAM(4,4'-dithiodipyridine)/Pd system [7]. Their successful approach consists of the complexation of Pd^{2+} ions at the nitrogen-containing top of SAM/Au followed by the reduction of $Pd^{2+} \rightarrow Pd^0$ in a solution free of Pd^{2+} ions in order to prevent the formation of the adsorption of Pd on the Au electrode [2, 3, 7–9]. The fact that the Pd layer is indeed deposited on top of the SAM and does not bind directly to the metal electrode was proven by cyclic voltammetry, *in situ* scanning tunneling microscopy (STM), *ex situ* angle-resolved X-ray photoelectron spectroscopy (XPS) and ultraviolet photoelectron spectroscopy (UPS) [2, 3].

Using STM, is has been shown that the structure of SAMs can be controlled by the choice of the particular ions in the solution [12, 13]. Yet, the interpretation of STM images is often not unambiguous. Here STM simulations based on first-principles electronic structure calculations can be rather helpful [14]. For a even more detailed characterization, the comparison of calculated and measured vibrational spectra of the adsorbed molecules [15] is rather useful. The structure of metallized SAMs, however, can not be assessed by STM techniques anymore since typically no atomic resolution of the metallic overlayer is possible. It has only been possible to show that regions of the SAMs not covered by a metallic overlayer after the metallization lose their perfect periodic arrangement. However, still measured valence band spectra of metal layers can be compared with calculated densities of states (DOS) [2, 3].

There have been already several theoretical studies addressing the structure of thiols adsorbed on noble metal surfaces based on density functional theory (DFT) [16]. Whereas many of these studies have focused on methylthiolate [17–21], also aromatic thiols have been considered [5, 14, 22–28]. At low coverages, the near bridge site has been found to be the most stable adsorption site for the smallest thioaromatics benzenethiol and 4-Mpy. The bridge site is also supposed to be most preferable in the denser structures, as was demonstrated [14] for 4-Mpy in the experimentally observed $7\times\sqrt{3}$ and $5\times\sqrt{3}$ structures on Au(111) [12, 13].

Motivated by recent experiments on the metallization of a 4-ATP self-assembled monolayer by a Pd overlayer [3] we have studied the Au/4-ATP/Pd system using periodic

DFT calculations. In a systematic approach we first addressed the structure of single 4-ATP molecules adsorbed on Au(111). Since SAMs are typically prepared in an aequeous evironment, we studied the interaction of adsorbed 4-ATP molecules with 1 to 9 water molecules. Finally, we determined the geometric and electronic structure of the Au/4-ATP/Pd system. Angle-resolved XPS measurements revealed that the 4-ATP SAM in the sandwich structure consists of two molecular layers [3]. Therefore we considered both a single and a double layer of 4-ATP between the Au(111) substrate and Pd layer and compared the calculated local density of states (LDOS) with UPS results.

II. COMPUTATIONAL DETAILS

All calculations were performed using the periodic DFT package VASP [29]. The exchange-correlation functional by Perdew, Burke and Ernzerhof (PBE) [30] was employed to describe the exchange-correlation effects within the generalized gradient approximation (GGA). The ionic cores were represented by projector augmented wave (PAW) potentials [31] as constructed by Kresse and Joubert [32]. The electronic one-particle wave function were expanded in a plane-wave basis set up to an energy cutoff of 400 eV.

4-aminothiophenol molecules adsorb as a thiolate, i.e. without the hydrogen atom of the S-H group. Therefore we refer the adsorption energy of 4-ATP on Au(111) to the free thiolate according to

$$\begin{aligned} E_{\text{ads}} &= E(\text{NH}_2\text{C}_6\text{H}_4\text{NS/Au(111)}) \\ &\quad -[E(\text{NH}_2\text{C}_6\text{H}_4\text{NS}) + E(\text{Au(111)})] \,, \end{aligned} \quad (1)$$

where $E(\text{NH}_2\text{C}_6\text{H}_4\text{NS/Au(111)})$, $E(\text{NH}_2\text{C}_6\text{H}_4\text{NS})$, and $E(\text{Au(111)})$ are the total energies of 4-ATP adsorbed on Au(111), the 4-ATP($\text{NH}_2\text{C}_6\text{H}_4\text{NS}$) radical in the gas phase, and the bare Au(111) surface, respectively. According to Eq. (1), exothermic adsorption is associated with a negative adsorption energy. In the following, we will refer to the *absolute* value of the adsorption energy as the binding energy. Note that in this energy balance the solvation energy of 4-ATP in the solution does not enter. However, taking this into account would only lead to a constant shift of all adsorption energies reported in this study but would not change the energetic ordering of the different considered structures.

The adsorption of isolated 4-ATP molecules on Au(111) was modeled within a 3×3 unit cell corresponding to a coverage of 1/9. If not specified differently, the surface is modeled by a slab of 5 Au layer. For the models containing Pd atoms, spin-polarization was allowed since Pd atoms in low-dimensional structures can become magnetic [33].

III. RESULTS

A. Adsorption of isolated 4-ATP molecules on Au(111)

To map out energy differences between stable and metastable complexes of a single 4-ATP on Au(111), geometry optimizations were performed for several initial arrangements with the S-head group of 4-ATP located at six non-equivalent sites on the (111) surface: top fcc, top hcp, fcc hollow, hcp hollow, near bridge fcc, and near bridge hcp, thereinafter abbreviated as t-fcc, t-hcp, fcc, hcp, b-fcc, and b-hcp, respectively (see Ref. [14] for a detailed description of the particular sites). The starting geometries involved various tilt angles between the S-C bond of 4-ATP and the Au(111) surface normal (denoted by θ_{Au-S-C}). The azimuthal angles were restricted to values of 0° and 180° corresponding to the $[1\bar{1}0]$ direction along one of the axes of the hexagonal surface unit cell of Au(111) which were found to be most stable for the similar aromatic thiolates benzothiolate [24] and mercaptopyridine [14]. Note that these two angles are not equivalent because of the tilted binding configuration of the aromatic molecules.

Table I summarizes the energy and structure parameters of isolated ATP on Au(111). The optimized 4-ATP/Au(111) complexes can be split into three groups according to the coordination of the sulfur head group: sulfur is bound to one, two, and three Au atoms at the top, near bridge, and hollow sites, respectively, which is illustrated in Fig. 1. Consequently, with increasing coordination number of S the length of the S-Au bond decreases and the angle θ_{Au-S-C} increases. Thus, ATP at the top sites forms the shortest S-Au bond with its aromatic ring almost parallel to the surface, whereas at the hollow sites the ring is oriented perpendicularly to the (111) plane. The most stable 4-ATP adsorption site is the bridge position whereas the hollow sites and top sites are about ~ 0.2 less stable but almost degenerate

TABLE I: Adsorption energies and geometry parameters for the 4-ATP molecule adsorbed at the top-fcc, top-hcp, hcp hollow, fcc hollow, bridge-hcp, and bridge-fcc sites of Au(111). $d_{\text{S-Au}}$ corresponds to the distance of the sulfur atom to the nearest Au atoms and $\theta_{\text{Au-S-C}}$ is the angle between the S-C bond of the 4-ATP molecule and the Au(111) surface normal.

Site	E_{ads} (eV)	$d_{\text{S-Au}}$ (Å)	$\theta_{\text{Au-S-C}}$ (°)
t-fcc	-1.043	2.43	72
t-hcp	-1.044	2.44	73
fcc tilted	-0.966	2.54 2.54 2.46	17
fcc upright	-0.987	2.47 2.47 2.49	1
hcp tilted	-0.910	2.74 2.74 2.53	48
hcp upright	-0.855	2.52 2.52 2.55	3
b-fcc	-1.206	2.51 2.51 *3.33*	60
b-hcp	-1.195	2.51 2.51 *3.34*	59

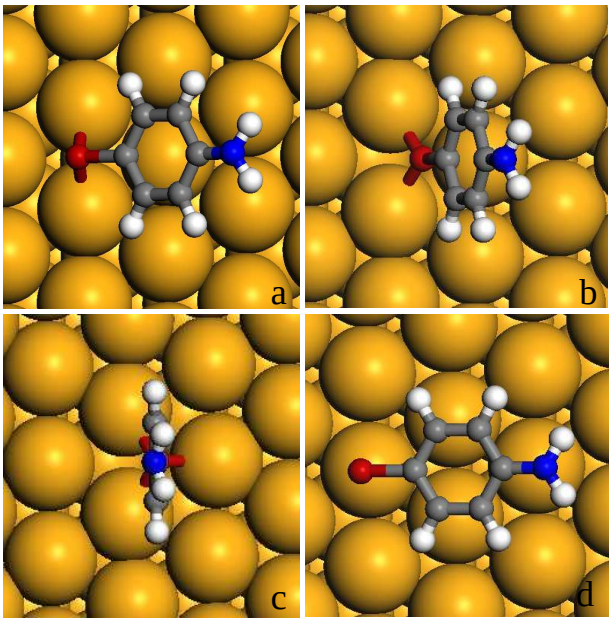

FIG. 1: Optimized structures of an isolated 4-aminothiophenol molecule adsorbed on a five-layer Au(111) slab within a 3×3 periodicity in the b-fcc (a), fcc tilted (b), fcc up-right (c), and t-fcc (d) configuration, respectively.

in energy. These structural and energetic features are typical for thioaromatics [14, 24].

The two different bridge configurations, b-fcc and b-hcp, are rather close in energy and have very similar structural parameters with the S-Au bonds having a length of 2.51 Å. Note that the displacement from the b-fcc to the b-hcp configuration involves a flipping in the angle θ_{Au-S-C}. The same is true for the change from the t-fcc to the t-hcp configuration. At the fcc and hcp hollow sites, there are several different local minima distinguished by different tilting angles θ_{Au-S-C} and moderately varying lengths of the S-Au bonds. The two local minima at the fcc site with tilt angles $\theta_{Au-S-C}\approx=17°$ (fcc tilted) and $\theta_{Au-S-C}\approx=1°$ (fcc upright) are practically energetically degenerate within the accuracy of our calculations whereas the hcp sites exhibit a slightly lower stability.

A comparison of our results for the adsorption of an isolated 4-ATP molecule with those found for 4-mercaptopyridine [14] and benzenethiol [24] on Au(111) shows rather similar values for the relative adsorption energies and the bonding geometries. This indicates that the S-Au bond is hardly affected by modifications of the benzene ring (all three molecules are built based on the skeleton of benzenethiol, they have the same local structure at the sulfur tail, only at the opposite tail either one carbon is replaced by a nitrogen atom (4-mercaptopyridine) or a hydrogen atom is substituted by an amino group (4-ATP).

We also checked whether an additional aromatic ring influences the S-Au bonding by performing DFT calculations for mercaptobiphenyl in the b-fcc, fcc up-right and t-fcc configurations using the same approach as for 4-ATP. In the configurations, we found S-Au bond lengths of 2.51, 2,48, and 2.42 Å at the b-fcc, fcc up-right, and t-fcc sites, respectively. The b-fcc configuration turned again out to be the most stable with the fcc (t-fcc) configuration being less stable by -0.177 (-0.189) eV. These findings follow practically the same trends as for the simpler thioaromatic presented above. However, for the denser structures one has to be aware that the mutual interaction between the aromatic molecules, mainly via van der Waals forces, also contributes to the adsorption energy. Thus the minimum energy structures of SAMs formed by thioaromatics with longer chains might differ from those formed by smaller molecules such as benzenethiolate of Mpy, where the S-Au bond dominates the total energy of the complex.

B. Influence of water on 4-ATP/Au complex

The SAMs formed by thiolates on Au(111) are in fact also stable at the solid-vacuum interface. However, the preparation of the SAMs or subsequent modification such as the metallization or functionalization of the molecules is typically done in an aqueous environment or in the presence of some other organic solvent. Often electrolytes are used containing solvated ions. Thus in the real preparation process there is a spectrum of various chemical species present which can interact with the molecules of the SAM. Naturally, the question arises about the effect of such interactions on the geometric and electronic properties and the stability (*e.g.* adsorption energies), structure, or electronic properties of SAM/metal complexes.

A completely realistic modelling of the SAM preparation process from first principles is computationally still not feasible and has to the best of our knowledge not done yet. Either one includes the effect of the environment in an approximate fashion, or one studies the effect of the different components of the environment on the stability of the SAMs individually. In this work, we performed first steps to assess the influence of the environment by studying the interaction of water molecules with a single 4-ATP molecule adsorbed on Au(111). To be specific, we focused on the strength of the interaction of water with the amino (NH_2) and S-head group of 4-ATP adsorbed on Au(111) and its consequences of the geometric and electronic structure of the 4-ATP/Au(111) complex, in particular as far as the S-Au bonding is concerned.

In a first step, we studied the interaction of water with the amino group of the 4-ATP molecule adsorbed on Au(111) *via* a hydrogen bond (H-bond) between a hydrogen atom of a water molecule (denoted by H_w in the following) and the nitrogen atom of the amino group (see Fig. 2 a-c). in the b-fcc and fcc up-right configuration within a 3×3 surface unit cell. The strength of the H-bond, reflected in the interaction energy defined as E_{int}=E(H_2O/4-ATP/Au)-

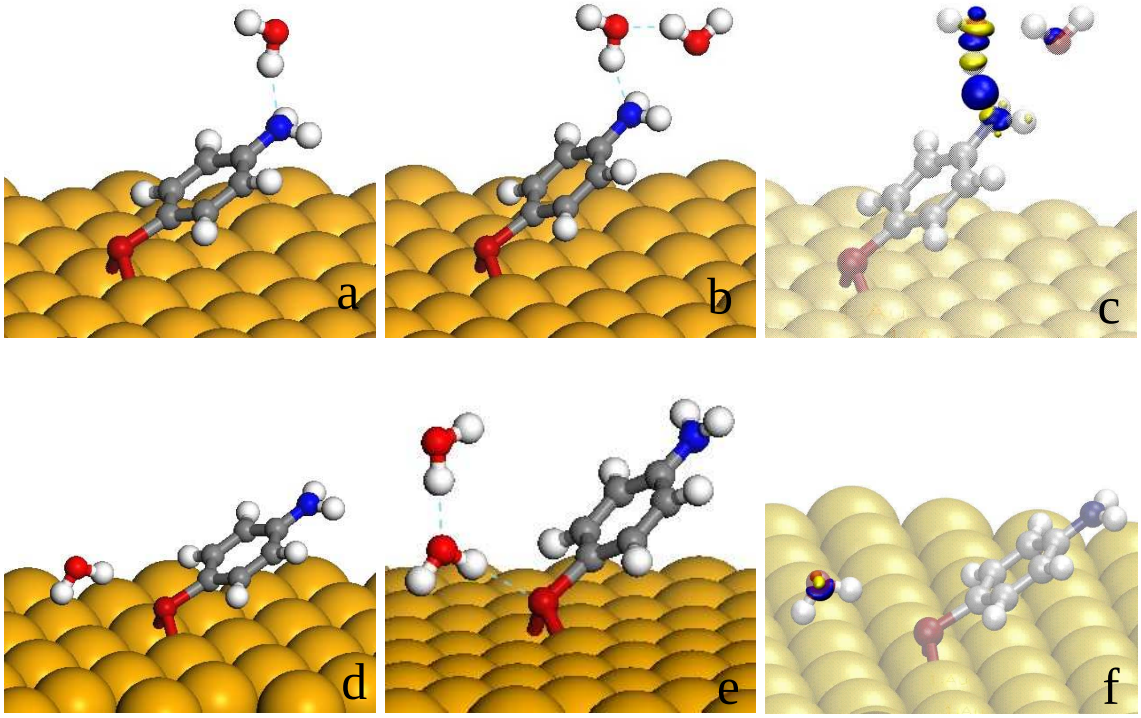

FIG. 2: Optimized structures of water molecules interacting with 4-ATP at the b-fcc site on Au(111): a) single water molecule forming a H-bond with the nitrogen atom of ATP, b) structure (a) with an additional water molecule added, c) isosurfaces of charge density differences for the configuration shown in (b), d) single water molecules interacting with the S-head group of ATP, e) structure (d) with an additional water molecule added, f) isosurfaces of charge density differences for the configuration shown in (d). In the charge density plots, blue and yellow surfaces depict areas of the electron accumulation and depletion, respectively. Note that in both cases, there are hardly any changes in the region of S-Au bond. The structures (a) and (b) were evaluated within a 3×3 periodicity, (d) and (e) within a 4×4 periodicity.

(E(4-ATP/Au)+E(H_2O), is -0.169 eV in the b-fcc and -0.209 eV in the fcc up-right configuration. In spite of the fact that the interaction is weaker in the b-fcc configuration, the length of the H-bond is almost identical in both geometries (2.02 and 2.03 Å in the b-fcc and the fcc up-right configuration, respectively).

In order to assess the consequences of the H-bond formation at the amino group on the structure of the adsorbed 4-ATP, both the relaxation energy (E_{rel}) and the change in the S-Au bond length were determined. E_{rel} is defined as the energy difference of the 4-ATP/Au complex in the fully optimized geometries without and with water. It amounts only to 7 and 8 meV in the b-fcc and the fcc configuration, respectively. Furthermore, there is no discernable shift in the S-Au length. Obviously, the formation of the N$\cdots$$H_w$ hydrogen bond has no effect on the stability of the 4-ATP/Au complex.

Admittedly, one single water molecule corresponds to a rather crude model of the water environment, in particular considering the fact that a NH_2 group can directly interact with three H_2O molecules. Thus, in a next step, we added a second H_2O molecule. The second water molecule induces a polarization typical for liquid water through the $H_2O\cdots H_2O$ interaction. Upon geometry optimization, the length of the N-H_w hydrogen bond decreased to 1.92 Å and the relaxation energy E_{rel} increased to 25 meV. This suggests a stronger interaction between polarized H_2O molecules and 4-ATP/Au compared to a single $H_2O\cdots$4-ATP/Au interaction. Still, the eventual elongation of the S-Au bond by 0.02 Å is far too small to indicate any significant influence on the S-Au bond. This is also confirmed by an analysis of the charge density difference $\Delta(\rho)$=ρ(H_2O/4-ATP/Au)-(ρ(4-ATP/Au)+ρ(4-ATP/Au)) plotted in Fig. 2c which does not show any charge density change in the region of the S-Au bond.

Next, we carried out an optimization of the 4-ATP/Au b-fcc complex interacting with one H_2O molecule *via* a S$\cdots$$H_w$ bond in a 4×4 periodicity (see Fig. 2 d). The optimized S-H_w distance is 2.74 Å (Fig. 2d). Again, the S-Au bond is hardly affected by the presence of the water molecules, as the charge density difference plot shown in Fig. 2f demonstrates.

The S-H_w distance is reduced to 2.35 Å after a second H_2O molecule is added, as shown in Fig. 2e. The decrease in the S-H_w distance implies that there is a stronger S$\cdots$

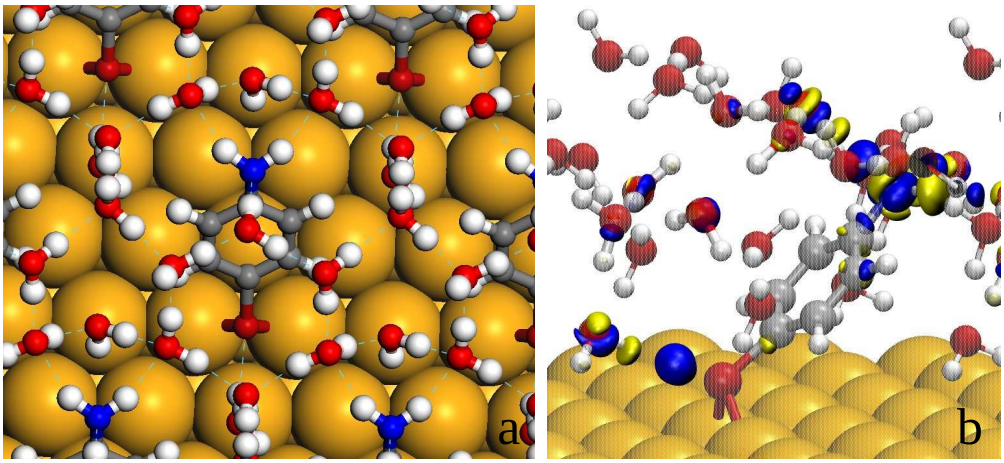

FIG. 3: An 4-ATP molecule on Au(111) in the b-fcc configuration surrounded by 9 water molecules in a 3×3 periodicity. a) Relaxed local minimum structure. The NH_2 group of 4-ATP directly interacts with three H_2O molecules. The distance of 4-ATP S-head group from the nearest hydrogen of a H_2O molecule is 2.36 Å. b) Change of the charge distribution induced by the presence of the water molecules in an isodensity representation. Blue and yellow surfaces correspond to charge accumulation and depletion, respectively. Note that there is hardly any change in the S-Au bond region.

$\cdot H_w$ interaction compared to the situation with only one H_2O molecule. This is due to the fact that H_w-O_w bond is weakened since the O_w is involved in a rather strong H-bond with the neighbouring H_2O molecule. However, also in this case there is only a negligible modification of the S-Au bond.

Finally, we deposited nine water molecules around the 4-ATP molecule in the b-fcc configuration on a three-layer Au(111) slab in a 3×3 periodicity. We selected an arrangement of H_2O molecules that included a H-bond between the nitrogen atom and H_w and two H-bonds between the hydrogen atoms of the NH_2 group (H_N) and the oxygen atoms of two H_2O molecules (O_w). The $9H_2O$/4-ATP/Au structure resulting after the geometry optimization is depicted in Fig. 3a.

The optimized H-bonds lengths are 1.94, 1.98, and 2.03 Å for the $H_w \cdots N$ bond and the two $H_N \cdots O_w$ bonds, respectively, whereas the length of the $S \cdots H_w$ bond is 2.36 Å. Although the relaxation energy is raised to $E_{rel} = 44$ meV, the S-Au bond length remains unchanged compared to the value for the isolated 4-ATP molecule in the b-fcc configuration. Thus the S-Au bond is unaffected by the presence of a complete water layer, as also confirmed by the charge density difference plot shown in Fig. 3b. It is true that we only considered one particular arrangement of the water molecules around the 4-ATP molecule on the Au(111) surface. Still, because of the fact that water is also relatively weakly interacting with metal substrates [34] it is rather improbable that the conclusions of this section, namely that the S-Au bond of adsorbed thiolates is hardly affected by the presence of water, will have to be changed because of some other water configuration.

C. Au/4-ATP/Pd sandwich structure

In this section, we will address the geometric and electronic structure of a molecular junction formed by a SAM made of 4-ATP molecules sandwiched between an Au(111) electrode and a Pd layer [3]. The Au-ATP and Pd-ATP contacts are made *via* S-Au and N-Pd bonds, respectively. We briefly summarize the experimental observations here: After formation of the 4-ATP SAM on Au(111), the Pd monolayer is deposited on top of the SAM in currentless Pd^{2+} complexation and electrochemical reduction ($Pd^{2+} \rightarrow Pd^0$) steps. The resulting Pd monolayer islands were characterized using STM, angle-resolved XPS and UPS [3]. The analysis revealed two facts. First, the metal-molecule system consists of an Au/4-ATP/Pd sequence rather than the thermodynamically more stable Au/Pd/4-ATP stacking, and second, the organic junction corresponds to two 4-ATP monolayers in between the Au electrode and the Pd layer.

In addition, the analysis of the Pd valence band spectra obtained by UPS indicated a drastic decrease of the density of states at the Fermi energy (E_F) compared to bulk Pd corresponding to a downshift by about 2 eV. First-principles calculations confirmed that such a large downshift cannot be explained as a consequence of a possible expansion of the Pd-Pd distance in the layer [2]. Rather, it was suggested that the downshift is due to covalent metal-molecule interactions [3].

In order to study the interaction of Pd atoms with the 4-ATP layer, we again followed a step-wise approach by first considering the bonding of a single Pd atom to an isolated 4-ATP/Au complex within a 3×3 surface unit cell and then looking at a Pd monolayer on-top of a $(\sqrt{3} \times \sqrt{3})$ R30° 4-ATP structure consisting of either one or two molecular layers. The Pd-N interac-

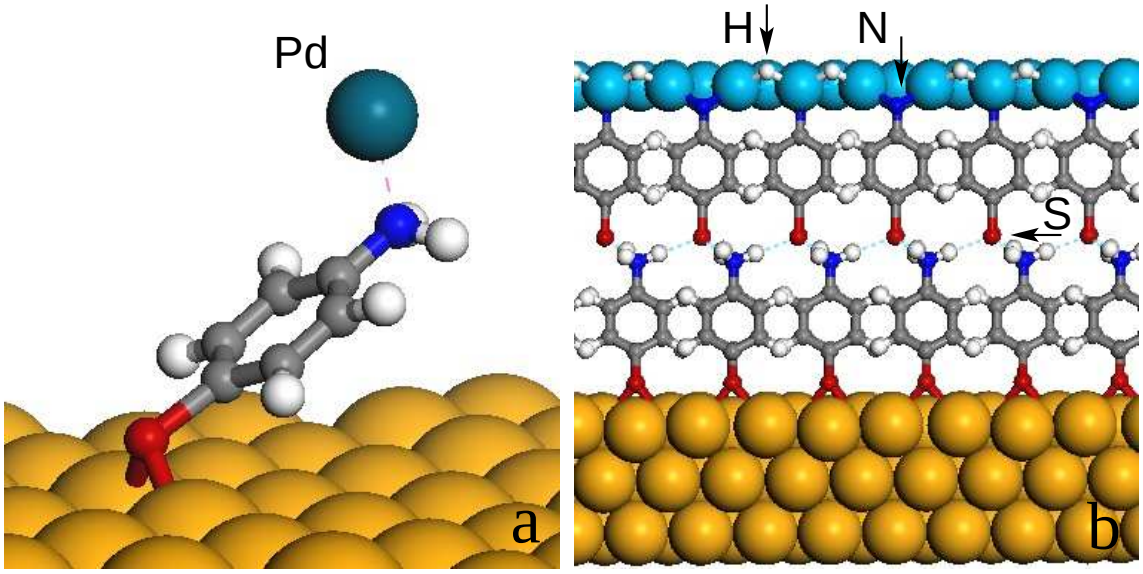

FIG. 4: Interaction of Pd with 4-ATP on Au(111). a) Optimized structure of a complex of a single Pd interacting with an isolated 4-ATP molecule at the b-fcc site of Au(111); b) The energectically most stable structure of two densely packed 4-ATP layer within a $\sqrt{3}\times\sqrt{3}$ periodicity sandwiched between the Au(111) substrate and a Pd monolayer. The amino groups of the 4-ATP molecules in the upper layer are dehydrogenated and the nitrogen atoms bind to three 3 Pd atoms. S- head group of a single 4-ATP from top most layer creates three H-bond with three -NH_3^+ group of the lower layer.

tion strength E_{int}=E(Au/4-ATP$_{isolated}$/1Pd)-(E(Au/4-ATP$_{isolated}$)+E(Pd)) was determined for isolated 4-ATP molecules in the b-fcc and fcc configuration, yielding very similar values of -1.01 and -0.98 eV, respectively, with an identical N-Pd bond lengths of 2.09 Å, but with S-Au bonds slightly elongated by 0.02 and 0.05 Å, respectively. Note that the interaction energies are about 0.5 eV weaker than in the case of a Pd atom interacting with 4-Mercaptopyridine/Au *via* a N-Pd bond. The Au/4-ATP/Pd complex at the b-fcc site (see Fig. 4a) is 0.25 eV more stable than at the fcc site. This energetic order is rather similar to the one without the Pd atoms (see Tab I) suggesting that the Pd$\cdots$4-ATP/Au bond does not modify the preference of the 4-ATP S-head group for a particular adsorption site on Au(111).

Finally, we modeled the whole Au/(4-ATP)$_n$/Pd junction, where $n = 1, 2$ corresponds to the number of 4-ATP layers, using a three-layer Au slab. The optimum structure with two 4-ATP layers is shown in a side view in Fig. 4b. For the structure of the 4-ATP SAM, we assumed a $\sqrt{3}\times\sqrt{3}$R30° arrangement, as suggested by earlier experiments [35]. This structure leads to an 4-ATP coverage on Au of 1/3, *i.e.* there is one 4-ATP molecule per three gold atoms in the substrate and accordingly also per three Pd atoms in the top layer. Note that in the periodic slab calculations, the spacing of the Pd atoms is given by the Au-Au distance in the substrate which means that the Pd layer is expanded by 5% with respect to bulk Pd [36]. This also means that no global relaxation of the Pd spacing is allowed.

The molecules of the first 4-ATP layer are bound to Au(111) in the b-fcc configuration. We first relaxed the geometry of the Au/4-ATP and Au/(4-ATP)$_2$ SAMs without the presence of Pd. The bonding geometry between the first and the second 4-ATP layer was adopted from the 4-ATP bulk structure with the S atom of the second 4-ATP layer bound to three lower lying 4-ATP molecules *via* three S-H hydrogen bonds (see Fig. 5).

The relaxed SAM structures then served as initial configurations for the geometry optimization of the molecular junctions Au/(4-ATP)$_n$/Pd (n=1,2). For the Pd layer, we assumed a densely-packed hexagonal structure bonded to the SAM via one-, two-, or three-fold coordinated N-Pd bonds. For both the one- and the two-layer 4-ATP model, the only stable configuration was the one with a single bond between the nitrogen atom and one Pd atom of the top layer at a distance of 2.1 Å. In order to check whether this preference for a single bond is a consequence of the expansion of the Pd layer, we evaluated the interaction of the N-tail of the 4-ATP molecule (NH_2-C_6H_4-SH) in a 3×3 periodicity with a free-standing Pd monolayer with Pd-Pd distances of 2.79 and 2.63 Å corresponding to the Pd-Pd separation in bulk and in a relaxed monolayer, respectively, as shown in Fig. 6a. For both Pd-Pd distances, a single N-Pd bond having a length of 2.2 and 2.1 Å, respectively, is the energetically most preferable bonding situation.

Note that as a consequence of the single bond between the SAM and the Pd monolayer the ratio of Pd atoms directly interacting Pd with the Pd layer via Pd-N bonds to noninteracting Pd atoms is 1/2. This has a significant influence on the electronic structure of the Pd layer,

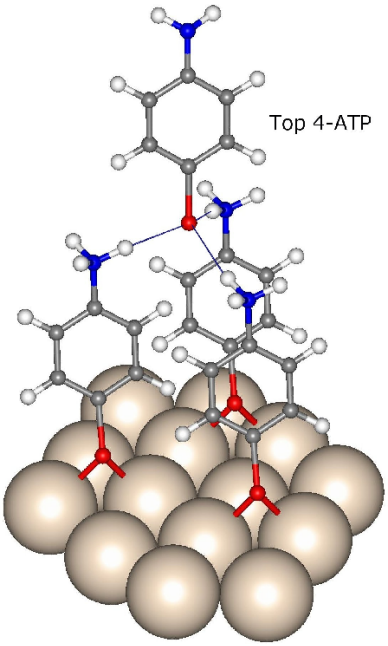

FIG. 5: Illustration of the bonding within the 4-ATP double layer structure. The sulfur head group of the 4-ATP molecules from the upper layer forms three hydrogen bonds with the amino groups of the lower layer.

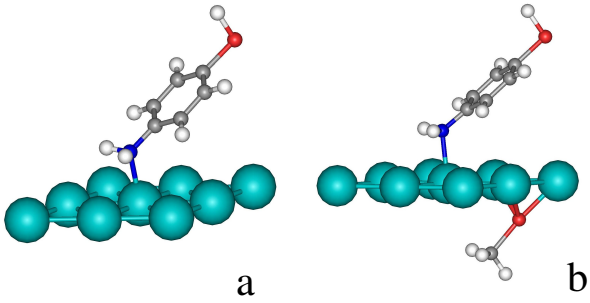

FIG. 6: Interaction of 4-ATP with a free-standing Pd monolayer. a) A single 4-ATP molecule (NH_2-C_6H_4-SH) interacts via a single bond between the nitrogen atom of 4-ATP and a Pd atom of the monolayer within a 3×3 periodicity. The 4-ATP molecule was kept in a C_{2v} symmetry. b) In addition to the 4-ATP molecule, a SCH_3 is adsorbed on the Pd monolayer at the other side within the 3×3 unit cell at a three-fold hollow position.

as the analysis of the calculated local density of states (LDOS) presented in the following will demonstrate. In order to facilitate the comparison with the UPS spectra obtained in the experiment [3], we convoluted the LDOS with a Gaussian of width 0.2 eV thus taking into account the finite energy resolution of the experimental spectra as well as the in general observed broadening of spectroscopic features due to the finite life time of the photoionized states.

In Fig. 7, calculated LDOS spectra of the Pd monolayer in the Au/$(4\text{-ATP})_2$/Pd junction in different configurations are plotted. The lowest curve corresponds to the spectra of the situation just discussed with a single Pd-N bond between the amino group of the 4-ATP molecule and the Pd monolayer. There is one prominent peak at -0.4 eV below E_F and two minor peaks at -1.6 and -2.8 eV. An analysis of the LDOS of the individual non-equivalent Pd atoms yields that the prominent peak stems from the Pd atoms not directly interacting with the 4-ATP molecule whereas the peak at -1.6 eV originates from the Pd atom bound via a single bond to the nitrogen atom. However, this spectrum is at variance with the experimental UPS spectrum that exhibits only one main peak at -1.8 eV and a strongly reduced intensity at the Fermi energy.

It is obvious that the discrepancy between theory and experiment is caused by the existence of Pd atoms not directly involved in bonding. Note that the experimental preparation of the M/SAM/M systems is carried out in an electrochemical environment that might contain additional sulfur- or nitrogen-containing molecules that would strongly bind to the Pd monolayer. Therefore we considered such additional adsorbates on top of the Pd layer. To be specific, we chose sulfur and nitrogen atoms and SCH_3 and NH_2CH_3 molecules to model the binding of sulfur- or nitrogen-containing molecules to Pd and determined their optimum adsorption structure.

In the stable configurations, S, N, and SCH_3 adsorb at the three-fold hollow position of the Pd layer whereas NH_2CH_3 forms a single bond to Pd above the top position. These site assignments were also checked for the free-standing Pd monolayer with reduced Pd-Pd distances (see Fig. 6b for the adsorption of methylthiolate (SCH_3) on the free-standing Pd monolayer).

The corresponding LDOS spectra are also included in Fig. 7. As a consequence of the additional interaction with the molecule, the first peak in the Pd LDOS below the Fermi energy is shifted down to values of -1.2, -1.6, -1.1, and -0.7 eV for the adsorbates S, N, SCH_3, and NH_2CH_3, respectively, also resulting in a reduction of the LDOS at the Fermi energy. Note that the smallest downshift is obtained for the singly bonded NH_2CH_3 molecule since for this adsorbate there is still on Pd atom left not directly interacting with any molecule. Still, for all these considered cases the agreement between the measured UPS spectrum and the calculated LDOS spectra is significantly improved. It follows that in order to interprete the electronic structure of the Pd layer deposited on top of the SAM it is important to take the possible bonding to molecules present in the solution into account. Since these molecules are strongly bound to the Pd monolayer, they will even persist under ultrahigh vacuum conditions.

On the other hand, one has to keep in mind that Pd is

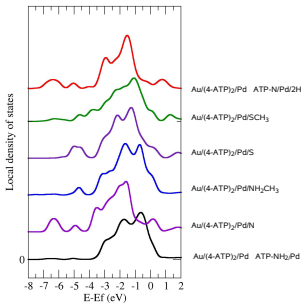

FIG. 7: Calculated local density of states (LDOS) of the Pd monolayer in the Au/(4-ATP)$_2$/Pd junction in various configurations and with additionally adsorbed atoms and molecules (see text).

also strongly interacting with hydrogen [37, 38]. Therefore we considered the case that the amino group of the 4-ATP molecule becomes dehydrogenated upon the formation of the metallic Pd layer with the hydrogen atoms being individually bound to the Pd layer. In such a situation that is depicted in Fig. 4b, the bare nitrogen atom forms three bonds to the metal atoms of the Pd layers. In fact, this configuration is about 1 eV more stable than the corresponding situation with the amino group still intact. Due to the fact that now every atom of the Pd layer is involved in the bonding to the underlying 4-ATP SAM, the Pd LDOS becomes strongly reduced at the Fermi energy with the first peak in the LDOS located at -1.6 eV, as shown in the top curve of Fig. 7, resulting in a very good agreement with the experiment [3].

Since the dehydrogenation of the amino group and the subsequent bonding of the individual hydrogen atoms to the Pd monolayer is strongly exothermic, we believe that this is the main cause for the downshift of the LDOS of the Pd monolayer metallized on top of the 4-ATP SAM. However, the calculations considering the adsorption of additional molecules on top of the Pd monolayer show that such adsorbates can also strongly contribute to the change in the Pd LDOS. In fact, this contribution might be more relevant in the formation of the Pd monolayer on top of a SAM made of 4-mercaptopyridine (4-Mpy) which exhibits a UPS spectrum [2] that is very similar to the one for the Au/(4-ATP)$_2$/Pd system. Since the nitrogen atom of 4-Mpy is a part of the aromatic ring, this atom can only form single bonds to metal atoms. Thus the reduction of the LDOS at the Fermi energy cannot be fully explained by a bonding of the nitrogen atom to the Pd layer, but rather the adsorption of additional molecules has to be involved.

IV. CONCLUSIONS

We have studied the geometric and electronic structure of Au(111)/4-aminothiophenol (4-ATP)/Pd molecular junctions using periodic density functional theory calculations. In a first step, we addressed the bonding of isolated 4-ATP molecules to Au(111). The most favorable adsorption configuration is at the near-bridge site with the sulfur head group in a twofold coordination, as for many other thiolates adsorbed on Au(111). Secondly, by including water molecules in the simulation cell, we found that the presence of water hardly affects the bonding of 4-ATP to the gold substrate which is of relevance since SAMs are typically prepared in an aqueous environment.

Finally, we studied the interaction of the Au/4-ATP system with Pd atoms. In the most stable configuration of the Pd monolayer ontop of an 4-ATP double layer, the amino groups of the upper 4-ATP layer become dehydrogenated and the bare nitrogen atoms bind to three Pd atoms. The strong Pd-N interaction leads to an reduced Pd density of states at the Fermi energy and a down-shift of the d-band, in agreement with the experiment. For an intact amino group, the interaction with the Pd layer is not only much weaker, but does also not reproduce the experimentally observed down-shift of the Pd d-band. However, sulfur- or nitrogen-containing adsorbates bound on top of the Pd layer could also lead to a strong modification of the Pd density of states.

Acknowledgments

Financial support by the Deutsche Forschungsgemeinschaft (DFG) within SFB 569 is gratefully acknowledged. We thank our colleagues H.-G. Boyen and D.M. Kolb for useful discussions. Computational resources have been provided by the bwGRiD project of the Federal State of Baden-Württemberg/Germany.

[1] J. C. Love, L. A. Estroff, J. K. Kriebel, R. G. Nuzzo, and G. M. Whitesides, *Chem. Rev.*, 2005, **105**, 1103–1169.
[2] H.-G. Boyen, P. Ziemann, U. Wiedwald, V. Ivanova, D. M. Kolb, S. Sakong, A. Groß, A. Romanyuk, M. Büttner, and P. Oelhafen, *Nature Mater.*, 2006, **5**, 394.
[3] M. Manolova, H.-G. Boyen, J. Kučera, A. Groß, A. Romanyuk, P. Oelhafen, V. Ivanova, and D. M. Kolb, *Adv. Mater.*, 2009, **21**, 320.
[4] A. Ulman, *Chem. Rev.*, 1996, **96**, 1533–1554.
[5] G. Heimel, L. Romaner, E. Zojer, and J.-L. Brédas, *Acc. Chem. Res.*, 2008, **41**, 721.
[6] M. Kind and C. Wöll, *Prog. Surf. Sci.*, 2009, **84**, 230.
[7] T. Baunach, V. Ivanova, D. M. Kolb, H.-G. Boyen, P. Ziemann, M. Büttner, and P. Oelhafen, *Adv. Mater.*, 2004, **16**, 2024.

[8] V. Ivanova, T. Baunach, and D. M. Kolb, *Electrochim. Acta*, 2005, **50**, 4283.

[9] M. Manolova, V. Ivanova, D. M. Kolb, H.-G. Boyen, P. Ziemann, M. Büttner, A. Romanyuk, and P. Oelhafen, *Surf. Sci.*, 2005, **590**, 146.

[10] O. Shekhah, C. Busse, A. Bashir, F. Turcu, X. Yin, P. Cyganik, A. Birkner, W. Schuhmann, and C. Wöll, *Phys. Chem. Chem. Phys.*, 2006, **8**, 3375–3378.

[11] F. Eberle, M. Manolova, D. M. Kolb, M. Saitner, H.-G. Boyen, J. Kučera, A. Groß, A. Romanyuk, and P. Oelhafen, Angew. Chem. Int. Ed. , accepted for publication.

[12] T. Baunach, V. Ivanova, D. A. Scherson, and D. M. Kolb, *Langmuir*, 2004, **20**, 2797.

[13] W. Zhou, T. Baunach, V. Ivanova, and D. M. Kolb, *Langmuir*, 2004, **20**, 4590.

[14] J. Kučera and A. Groß, *Langmuir*, 2008, **24**, 13985.

[15] I. Respondek and D. Benoit, *J. Chem. Phys.*, 2009, **131**, 054109.

[16] A. Groß, *J. Comput. Theor. Nanosci.*, 2008, **5**, 894.

[17] H. Kondoh, M. Iwasaki, T. Shimada, K. Amemiya, T. Yokoyama, T. Ohta, M. Shimomura, and S. Kono, *Phys. Rev. Lett.*, 2003, **90**, 066102.

[18] P. Maksymovych, D. C. Sorescu, and J. John T. Yates, *J. Phys. Chem. B*, 2006, **110**, 21161.

[19] P. Maksymovych, D. C. Sorescu, and J. John T. Yates, *Phys. Rev. Lett.*, 2006, **97**, 146103.

[20] M. Yu, N. Bovet, C. J. Satterley, S. Bengio, K. R. J. Lovelock, P. K. Milligan, R. G. Jones, D. P. Woodruff, and V. Dhanak, *Phys. Rev. Lett.*, 2006, **97**, 166102.

[21] R. Mazzarello, A. Cossaro, A. Verdini, R. Rousseau, L. Casalis, M. F. Danisman, L. Floreano, S. Scandolo, A. Morgante, and G. Scoles, *Phys. Rev. Lett.*, 2007, **98**, 016102.

[22] Y. Akinaga, T. Nakajima, and K. Hirao, *J. Chem. Phys.*, 2001, **114**, 8555–8564.

[23] J. Nara, S. Higai, Y. Morikawa, and T. Ohno, *J. Chem. Phys.*, 2004, **120**, 6705–6711.

[24] J. Nara, S. Higai, Y. Morikawa, and T. Ohno, *Appl. Surf. Sci.*, 2004, **237**, 433–438.

[25] A. Bilić, J. R. Reimers, and N. S. Hush, *J. Chem. Phys.*, 2005, **122**, 094708.

[26] S. Tanibayashi, T. Tada, S. Watanabe, and H. Sekino, *Chem. Phys. Lett.*, 2006, **428**, 367 – 370.

[27] R. B. Pontes, F. D. Novaes, A. Fazzio, and A. J. R. Da Silva, *J. Am. Chem. Soc.*, 2006, **128**, 8996–8997.

[28] G. Heimel, L. Romaner, J.-L. Brédas, and E. Zojer, *Surf. Sci.*, 2006, **600**, 4548.

[29] G. Kresse and J. Furthmüller, *Phys. Rev. B*, 1996, **54**, 11169.

[30] J. P. Perdew, K. Burke, and M. Ernzerhof, *Phys. Rev. Lett.*, 1996, **77**, 3865.

[31] P. E. Blöchl, *Phys. Rev. B*, 1994, **50**, 17953.

[32] G. Kresse and D. Joubert, *Phys. Rev. B*, 1999, **59**, 1758.

[33] A. Groß, *Theoretical surface science – A microscopic perspective*, Springer, Berlin, 2nd ed., 2009.

[34] Y. Gohda, S. Schnur, and A. Groß, *Faraday Discuss.*, 2009, **140**, 233–244.

[35] Y.-T. Kim, R. L. McCarley, and A. J. Bard, *J. Phys. Chem.*, 1992, **96**, 7416.

[36] A. Roudgar and A. Groß, *J. Electroanal. Chem.*, 2003, **548**, 121.

[37] W. Dong, V. Ledentu, P. Sautet, A. Eichler, and J. Hafner, *Surf. Sci.*, 1998, **411**, 123.

[38] M. Lischka and A. Groß, *Phys. Rev. B*, 2002, **65**, 075420.